

Research Articles | Behavioral/Cognitive

## Post-Ictal Sleep Changes in Human Focal Epilepsy

<https://doi.org/10.1523/JNEUROSCI.0303-25.2026>

Received: 12 February 2025

Revised: 30 December 2025

Accepted: 23 January 2026

Copyright © 2026 the authors

---

*This Early Release article has been peer reviewed and accepted, but has not been through the composition and copyediting processes. The final version may differ slightly in style or formatting and will contain links to any extended data.*

**Alerts:** Sign up at [www.jneurosci.org/alerts](http://www.jneurosci.org/alerts) to receive customized email alerts when the fully formatted version of this article is published.

# Post-Ictal Sleep Changes in Human Focal Epilepsy

Vaclav Kremen<sup>1,2,†</sup>, Vladimir Sladky<sup>1,2†</sup>, Vaclav Gerla<sup>2,†</sup>, Yurui Cao<sup>1,3</sup>, Filip Mivalt<sup>1</sup>, Erik K. St. Louis<sup>1</sup>, Mark R. Bower<sup>4</sup>, Ben Brinkmann<sup>1</sup>, Kai Miller<sup>5</sup>, Jamie VanGompel<sup>5</sup>, Mark Cook<sup>6</sup>, Tim Denison<sup>7</sup>, Kent Leyde<sup>8</sup>, Gregory A. Worrell<sup>1</sup>

<sup>†</sup>These authors contributed equally to this work.

## Author affiliations:

1 Department of Neurology, Mayo Clinic, Rochester, 55905, MN, USA

2 Czech Institute of Informatics, Robotics, and Cybernetics, Czech Technical University in Prague, Prague, 16000, Czech Republic

3 Department of Electrical & Computer Engineering, University of Illinois, Urbana Champaign, IL, USA

4 Department of Neurology, Yale University, New Haven, CT, USA

5 Department of Neurologic Surgery, Mayo Clinic, Rochester, 55905, MN, USA

6 St. Vincent's Hospital and University of Melbourne, Melbourne, Australia

7 Department of Engineering Sciences, Oxford University, Oxford, UK

8 Cadence Neuroscience, Seattle, WA, USA

**Correspondence to:** Vaclav Kremen and Gregory A. Worrell

Full address 200 First Street SW, Rochester, MN, 55905, USA

E-mail [kremen.vaclav@mayo.edu](mailto:kremen.vaclav@mayo.edu) and [worrell.gregory@mayo.edu](mailto:worrell.gregory@mayo.edu)

**Abbreviated title:** Post-Ictal Sleep Changes in Human

**Keywords:** Focal epilepsy; Slow wave sleep; Local field potentials; Sleep-wake states; Sleep architecture; Seizure-related consolidation.

Number of pages = 24; Number of figures = 6; Number of tables = 5; Number of multimedia = 0; Number of 3D models = 0; Number of words for abstract = 199; introduction = 649; discussion = 463.

## Acknowledgements

This research was supported by the US National Institutes of Health: UH2/UH3-NS95495 and R01-NS09288203. This scientific article is part of the CLARA project that has received funding from the European Union's HORIZON EUROPE research and innovation programme under Grant Agreement No 101136607. The implanted devices were donated by

33 Medtronic Plc. as part of the National Institutes of Health Brain Initiative. The authors thank  
34 the people with epilepsy for participating in this research. We thank Certicon a.s. for the use  
35 of CyberPSG tool for the visual review of EEG.

## 36 **Conflict of interest**

37 G.A.W., V.S., V.K., and B.H.B. declare intellectual property disclosures related to behavioral  
38 state and seizure classification algorithms. G.A.W., B.H.B and J.V.G declare intellectual  
39 property licensed to Cadence Neuroscience Inc. G.A.W. and J.V.G have licensed intellectual  
40 property to NeuroOne, Inc. G.A.W. is an investigator for the Medtronic Deep Brain-  
41 Stimulation Therapy for Epilepsy Post-Approval Study. M, C. is chief medical officer at  
42 Epiminder Inc., T.D. is co-founder and the Chief Engineer at Amber Therapeutics. K.L is co-  
43 founder and the chief executive officer at Cadence Neuroscience, inc. The remaining authors  
44 declare that they have no competing interests.

45

## 46 **Abstract**

47 Bidirectional interactions between sleep, seizures, and epilepsy remain incompletely  
48 understood. Evidence from animal models and people with focal epilepsy suggest that  
49 seizures may engage mechanisms of memory consolidation during post-ictal sleep to  
50 reinforce and strengthen synaptic connections within the pathological networks that  
51 generates seizures, termed seizure-related consolidation (SRC). Human studies of post-ictal  
52 sleep changes supportive of SRC, however, are limited by small sample size and restricted  
53 observations of post-ictal sleep. We investigated the interplay between seizures and sleep  
54 by analyzing sleep-wake and seizure catalogs derived from continuous local field potential  
55 (LFP) recordings in 11 people (6 males and 5 females) with drug-resistant focal epilepsy  
56 implanted with novel investigational devices and living in their natural environments. Our

57 findings demonstrate that post-ictal rapid-eye-movement sleep duration is reduced, whereas  
58 slow-wave sleep duration, slow-wave LFP spectral power and waveform slope are increased  
59 compared to inter-ictal nights without preceding seizures. The most significant changes  
60 localize to the epileptogenic networks generating the participants' habitual seizures. These  
61 results reveal parallels between SRC and physiological memory consolidation, providing  
62 novel insights into the potential role of post-ictal sleep in strengthening epileptic neural  
63 engrams, and may have implications for targeted disruption of post-ictal sleep and SRC in  
64 focal epilepsy.

## 65 **Significance Statement**

66 This study uses long-term intracranial local field potential (LFP) recordings to investigate the  
67 relationship between seizures and sleep in epilepsy. The post-ictal slow-wave sleep  
68 duration, spectral power, and waveform slope are increased compared to inter-ictal. Post-  
69 ictal rapid-eye-movement sleep duration is reduced. These changes are most significant  
70 within the epileptogenic networks that generate the participants habitual seizures. While this  
71 study cannot directly elucidate the mechanism involved in post-ictal sleep modulation, the  
72 study results are consistent with post-ictal sleep reinforcing pathological seizure networks  
73 through a process similar to physiological memory consolidation, here termed seizure-  
74 related consolidation (SRC). These results provide novel insights into the potential role of  
75 post-ictal sleep in epilepsy, with implications for potential targeted disruption of post-ictal  
76 sleep and SRC.

## 77 **Introduction**

78 Sleep is essential for brain health and facilitating learning and memory (Huber et al. 2004;  
79 Klinzing, Niethard, and Born 2019). Sleep is often disrupted in neurological and psychiatric  
80 disorders, but distinguishing whether sleep directly mediates brain dysfunction or simply  
81 reflects disease changes remains challenging. Leveraging long-term monitoring in

82 individuals living in their natural environment has strengthened the connection between poor  
83 sleep and chronic medical conditions, underscoring the potential of sleep as a therapeutic  
84 target (Zheng et al. 2024).

85

86 In epilepsy, the interplay between seizures and sleep has long intrigued clinicians and  
87 researchers (Gowers 1885). However, most studies utilizing invasive brain recording are  
88 relatively short, multi-day recordings during inpatient hospital settings and inherently limited  
89 for investigating the longitudinal interplay between seizures and sleep (Peter-Derex et al.  
90 2020). Growing evidence supports reciprocal sleep-epilepsy relationships, with sleep  
91 disturbances increasing seizures (Bazil 2017) and seizures disrupting sleep architecture,  
92 including spindles and slow-wave activity (Boly et al. 2017).

93

94 Beyond acute seizure events, long-term pathological changes in synaptic connectivity—a  
95 hallmark of epileptogenesis—are believed to be a central mechanism in epilepsy  
96 progression. In animal models, epileptic activity directly competes with normal plastic  
97 changes required for memory formation (Ferrero et al. 2025). Similarly, people with epilepsy  
98 often exhibit impaired memory formation that scales proportionally with their overall seizure  
99 burden (Hermann et al. 2020). The concept of seizure-related consolidation (SRC) posits  
100 that recurrent seizures exploit the mechanisms of memory formation, acting as powerful  
101 “engrams” to strengthen pathological networks (Goddard and Douglas 1975; M. Bower et al.  
102 2015; M. R. Bower et al. 2017; M. R. Bower 2024) and alters sleep homeostasis. Evidence  
103 of seizure reactivation and consolidation has been observed in individuals with temporal lobe  
104 epilepsy (M. R. Bower et al. 2017; M. Bower et al. 2015) supporting parallels between SRC  
105 and physiological memory mechanisms. Electrophysiological biomarkers, including inter-ictal  
106 epileptiform spikes (IES), high-frequency oscillations, and seizures, may represent powerful,  
107 pathological epileptic engrams. These biomarkers are increasingly seen as potential targets

108 for therapeutic interventions aimed at disrupting SRC processes (Hsu et al. 2008; M. Bower  
109 et al. 2015; Ferrero et al. 2025).

110

111 While promising, the investigation of SRC and its relationship with sleep in ambulatory  
112 humans is hindered by the inaccuracy of self-reported seizure and sleep diaries (Lauderdale  
113 et al. 2008; Elger and Hoppe 2018). To address these challenges, we developed machine  
114 learning (ML) frameworks for classifying sleep-wake states and detecting seizures from  
115 continuous intracranial local field potential (LFP) recordings. The ML algorithms are applied  
116 to long-term LFP data from investigational devices implanted in individuals with focal  
117 epilepsy and provide accurate sleep-wake and seizure classification catalogs (Kremen et al.  
118 2019; Sladky et al. 2022; Mivalt et al. 2022). We previously used these ML classification  
119 algorithms to demonstrate the role of sleep-wake states in multiscale cycles of seizures, IES,  
120 mood, impedance, and seizure forecasting (Dell et al. 2021; Mivalt, Kremen, et al. 2023;  
121 Kremen et al. 2025).

122

123 A particularly interesting finding in our previous studies was that individuals experience  
124 longer sleep durations on nights following seizures (Dell et al. 2021). Given sleep's  
125 established role in learning and memory (Diekelmann and Born 2010; Walker and Stickgold  
126 2010), this aligns with the hypothesis that post-ictal sleep facilitates the SRC process. Scalp  
127 EEG studies are also consistent with this observation, demonstrating increased post-ictal  
128 non-REM (NREM) sleep duration, slow-wave activity (SWA), and waveform slope following  
129 focal to bilateral tonic-clonic seizures (Boly et al. 2017).

130

131 In the current study, chronic intracranial LFP recordings from people with focal epilepsy  
132 show increased post-ictal slow-wave sleep duration, SWA spectral power and waveform  
133 slope. Interestingly, the post-ictal REM durations are decreased, consistent with previously

134 reported findings epilepsy monitoring unit studies (Bazil, Castro, and Walczak 2000; Nobili et  
135 al. 2025). In summary, the novel long-term LFP data support a possible role for SRC in  
136 human epilepsy and highlight the potential of targeting interventions (Ferrero et al. 2025; Lai  
137 et al. 2024) to disrupt post-ictal NREM sleep and SRC.

## 138 **Materials and Methods**

### 139 **Experimental Design and Statistical Analyses**

#### 140 **Human Participants**

141 We analyzed two cohorts (cohorts #1 & #2) of human participants with drug-resistant focal  
142 epilepsy implanted with investigational devices providing continuous local field potential  
143 (LFP) sensing from multiple brain regions (Figure 1A and Figure S1).

144 Cohort #1 (NC) includes continuous, long-term LFP data from participants implanted with the  
145 investigational seizure advisory system (NeuroVista Inc.) between March 24, 2010, and June  
146 21, 2011 in Melbourne, Australia (Cook et al. 2013). Seizure onset networks included  
147 neocortical temporal, frontal, and parietal brain regions (Table 1). Participants were  
148 implanted with four subdural, 4-contact, cortical strip electrode arrays over the region of the  
149 seizure focus. The subdural arrays were connected to lead extensions tunneled down the  
150 neck to an implantable subclavicular LFP recording and telemetry unit. The LFP data were  
151 wirelessly transmitted to a hand-held device running algorithms to detect and forecast  
152 seizures (Cook et al. 2013). Due to various technical factors, the NC cohort suffers from  
153 substantial data loss, which potentially limits the scope of our analysis. Consequently, we  
154 introduced quantifiable metrics to delineate subjects into inter-ictal and post-ictal  
155 groups (Figure 1D): 1.) each participant contributed  $\geq 10$  days of continuous LF recordings  
156 in each period covering both interictal nights (no seizures for at least 48 (NC cohort) or 24h

157 (mT cohort) before the night) and postictal night (first night within 24h after a seizure)  
158 periods. 2.) For each participant, we included only days where  $\geq 80\%$  of the total recording  
159 time during the night was successfully recorded. 3.) No missing data either at the beginning  
160 or ends of the sleep/nights. Using above criteria, we were able to identify six participants  
161 from the NC cohort (5 males and 1 female). We report average data rate in 24-hour day  
162 cycle for each NeuroVista participant in Figure S2 in supplementary data (including six  
163 selected participants for our study). We show an example of one week data for NC-2  
164 participant with seizures, hypnogram, and electrophysiological features of LFP to  
165 demonstrate how sleep scoring reflects power in bands, and the challenge to select interictal  
166 data (Figure S3). The opposite scenario can happen with rare seizure occurrence making  
167 selection of postictal data challenging. Also note that most of the seizures happen during  
168 Awake behavioral state.

169 Cohort #2 (mT) includes continuous, LFP data from 5 participants (1 male and 4 females) in  
170 a clinical trial using the investigational Medtronic Summit RC+S™ between July 10, 2019  
171 and October 23, 2023 at Mayo Clinic, MN, USA (Table S2) (Kremen et al. 2024). All  
172 participants had bilateral amygdala-hippocampus onset seizures (Table 1). Four leads with  
173 4-electrode contacts targeted the bilateral amygdala-hippocampus and anterior nucleus of  
174 thalamus. Lead extensions were tunneled down the neck to a subclavicular rechargeable,  
175 electrical stimulation, LFP sensing, and wireless telemetry device (Figure 1A). The LFP data  
176 were wirelessly streamed to a cloud storage using BrainRISE, a platform ecosystem for  
177 automatic data capture and automated data analysis (seizure and spike detection, sleep  
178 scoring, and participant reporting) (Sladky et al. 2022; Kremen et al. 2025; Mivalt et al.  
179 2022).

180 The neocortical epilepsy participants (NC 1-6) had electrode contacts in the neocortex  
181 targeting seizure onset zone (SOZ) and outside the seizure onset zone (NSOZ). The  
182 participants with mT (mT 1-5) had bilateral independent seizures recorded from electrodes in  
183 epileptogenic hippocampus bilaterally. Data from these 11 participants was used for the

184 evaluation of sleep duration, sleep architecture, and slow-wave LFP spectral power and  
185 waveform slope. We analyzed SOZ and NSOZ contacts to investigate electrophysiological  
186 differences in the brain regions generating seizures in the neocortical epilepsy participants.

187 All participants from NC and mT cohort provided informed consent for device implantation  
188 and research participation, and human subjects research approval was provided by the  
189 respective institutional review boards based at University of Melbourne (NC) and Mayo Clinic  
190 (mT).

## 191 **Intracranial Electrophysiology Recordings**

192 The LFP were continuously recorded from multiple brain structures using the NeuroVista and  
193 RC+S™ devices (Figure 1). The NeuroVista device recorded 16 channels of subdural LFP  
194 data using an average reference (calculated from the 16 contacts) and sampled at 400 Hz  
195 (bandwidth 0.85 – 100 Hz) from temporal, frontal, and parietal neocortex. For the NC cohort,  
196 we separated electrodes into two groups: Seizure Onset Zone (SOZ) electrodes versus non-  
197 SOZ (NSOZ) electrodes. Electrodes were classified based on the seizure onset within a 1-  
198 second onset window.

199

200 The RC+S™ device recorded four bipolar LFP channels sampled from the 16 parenchyma  
201 electrode contacts in the bilateral anterior nucleus of the thalamus (ANT), amygdala (AMG),  
202 and hippocampus (HPC). The LFP was sampled at 250 Hz (bandwidth 0.85 – 80 Hz). Long-  
203 term recordings from the 5 participants included at least 1 month of LFP data.

204 The analysis encompassed a combined dataset of **1,501 day-nights** of chronic recordings  
205 drawn from both cohorts.

## 206 **Automated Seizure Detection**

207 We used an automated deep learning model (convolutional neural network with long short-  
208 term memory: CNN-LSTM) to label candidate seizures (Sladky et al. 2022). The CNN-LSTM  
209 seizure detector was developed and validated previously within a complex study with  
210 sensing devices implanted in naturally occurring canine and human epilepsy. Long-term  
211 records from humans and canines with epilepsy living in their natural environments provided  
212 a large data set of spontaneously occurring seizures. These datasets are highly imbalanced  
213 because seizures are relatively rare events when compared to the continuous inter-ictal LFP  
214 data. The CNN-LSTM seizure detector represents a technological evolution from early  
215 seizure detectors based on hand-crafted features and traditional machine learning to modern  
216 methods employing deep learning for automated feature extraction (Nejedly et al. 2019;  
217 Sladky et al. 2022). The full performance analysis, including the sensitivity and specificity of  
218 the CNN-LSTM seizure detector when applied to this study cohort, is tested by Sladky  
219 (Sladky et al. 2022) showing AUROC 0.97+/-0.03 on NC dataset and 0.99+/-0.01 on mT  
220 dataset.

221 In this study the detector's performance, was optimized for high sensitivity and generated a  
222 set of candidate seizure detections. These candidate detections were visually reviewed by  
223 an epileptologist to accurately identify and annotate true seizures, leveraging the detector's  
224 high sensitivity to minimize the risk of missing seizure events.

## 225 **Automated Behavioral State Classification**

226 We classified sleep-wake states using our previously developed automated machine  
227 learning (ML) framework for LFP-based behavioral state classification (Kremen et al. 2019,  
228 2017; Mivalt et al. 2022). This framework in general enables unsupervised, semi-supervised,  
229 and supervised learning to classify the behavioral state: Awake, NREM (N2 and N3 ),  
230 and REM(Kremen et al. 2019). The general approach employs a human expert-in-the-loop  
231 ML paradigm, training and testing on invasive LFP recordings simultaneous  
232 with polysomnography (PSG) scored against AASM criteria (Silber 2012). The validity of the

233 LFP-based classification against gold-standard scalp PSG has been previously established  
234 (Kremen et al. 2019, 2017; Mivalt et al. 2022).

235 For the medial mT cohort, we utilized the classifier reported previously by Mivalt et al. (Mivalt  
236 et al. 2022). The performance metrics for this specific dataset were: overall -score of  
237 0.90 (NREM -score: 0.94; REM -score: 0.67; Awake -score: 0.83), and have been used in  
238 prior analyses of the mT cohort (Mivalt et al. 2022; Kremen et al. 2025; Mivalt, Sladky, et al.  
239 2023).

240 For the NC cohort, we implemented the unsupervised classification framework originally  
241 developed and validated on subjects with intracranial electrodes implanted for epilepsy  
242 evaluation (Kremen et al. 2019). Given that the NC dataset consisted only of  
243 neocortical electrodes (lacking the depth electrodes included in the original validation  
244 cohort (Kremen et al. 2019)), we retested the published unsupervised method (Kremen et al.  
245 2019, 2017) to include REM sleep and suitability for transfer to the NC cohort. This retesting  
246 involved applying the approach exclusively to data from the neocortical channels of a  
247 combined cohort in Kremen et al. (Kremen et al. 2019) (LFP recorded with iEEG using grids  
248 and strips only, scalp EEG, and gold-standard PSG annotations), selecting electrode for  
249 sleep scoring for each available patient, annotate data based on EEG features, train the  
250 classifier, and test/compare the classifier to a gold standard labels. This modified approach  
251 yielded an overall accuracy of 0.87 and an estimated  $F_1$  score of 0.82 for Awake,  $F_1 = 0.87$   
252 for REM, and  $F_1=0.65$  for REM, which supports suitability for transfer to the NC data, despite  
253 being slightly lower than the original published results that incorporated sEEG electrodes  
254 (Kremen et al. 2019, 2017). Final results of the sleep classification for the NC data were  
255 used in previous published studies (Dell et al. 2021; Payne et al. 2021).

## 256 **Electrophysiological Features**

257 The LFP data from subdural strips and penetrating parenchyma electrodes were exported as  
258 Multiscale Electrophysiology Format (MEF

259 [https://www.mayo.edu/research/labs/bioelectronics-neurophysiology-engineering/data-code-](https://www.mayo.edu/research/labs/bioelectronics-neurophysiology-engineering/data-code-sharing)  
260 [sharing](https://www.mayo.edu/research/labs/bioelectronics-neurophysiology-engineering/data-code-sharing)) files and analyzed using custom algorithms developed in Python programming  
261 language (Python 3.8) to characterize LFP features similar to work by Carvalho et al.  
262 (Carvalho et al. 2024). Spectral power in all channels was obtained for specific frequency  
263 bands of interest in each 30-sec epochs following a previously described approach using  
264 Fast Fourier Transform (Kremen et al. 2017), and consistent with previous literature (Varga  
265 et al. 2016; Marshall et al. 2006). We first applied a bandpass finite impulse response (FIR)  
266 filter with zero-phase-shift to bandpass signal in the 0.5 - 35 Hz band to extract spectral  
267 power features. The filter length was 2000, and we used a hamming window design method.  
268 A power spectral density related to SWA was calculated in Delta band (1 - 3 Hz). We  
269 summarized the data by calculating the mean Delta Power across all visually scored NREM  
270 sleep epochs.

271 We obtained SWA down slopes similar to those of other authors (Riedner et al. 2007;  
272 Jaramillo et al. 2020). For artifact-free NREM data segments, we first filter the signal by a  
273 bandpass FIR filter with zero phase shift into 0.5 – 35Hz band (same as above). Like  
274 Riedner, subsequently, we apply a 50-millisecond moving average filter. Then, we detect  
275 zero crossings of the signal and select the descending segments of negative half-waves  
276 whose zero crossings were separated by 0.25 to 1.0 seconds for slow waves. We followed  
277 the approach similar to Achermann et al. (Bersagliere and Achermann 2010) with filter  
278 amplitude set at +/- 5  $\mu$ V to eliminate waveforms we did not feel confident represented SWA.  
279 As discussed by multiple authors in PSG slow wave literature, setting higher amplitude filters  
280 is a significant problem in older adult subject due to smaller amplitudes of waveforms, which  
281 can lead to bias. Moreover, both Achermann's and Riedner's studies showed that small or no  
282 amplitude cut-off SWs are homeostatically regulated and may be more sensitive than  
283 applying amplitude thresholds(Bersagliere and Achermann 2010). Subsequently,  
284 we automatically identified troughs of slow waves after each zero-crossing on the signal.  
285 And as a final step, we divide the amplitude difference (in  $\mu$ V) (descending negative slope)

286 by their interval (time difference between them in seconds). Summary slope metrics were  
287 obtained by averaging each slow wave slope in delta bands in each 30-second epoch and  
288 then across all NREM epochs, generating a mean positive and negative delta-slope estimate  
289 during NREM sleep for each electrode (Fig 1D).

290 We implemented the algorithm and provided examples of its use and documentation in the  
291 Behavioral State Analysis Toolbox (BEST) (<https://github.com/bnelair/best-toolbox>), a  
292 Python package for behavioral state analysis using EEG. BEST includes tools for automated  
293 sleep classification of long-term iEEG data recorded using implantable neural stimulation  
294 and recording devices, removal of DBS artifacts, and feature extraction from the EEG data,  
295 now including delta and slow oscillation slopes. The tools were developed in  
296 the [Bioelectronics Neurophysiology and Engineering Laboratory](#) at Mayo Clinic, Rochester,  
297 MN, USA. The codes for the analysis pipeline above and one specific example of using it  
298 one patient and in single night, including the data, can be found at:

299 [https://github.com/bnelair/best-toolbox/blob/master/projects/slow\\_wave\\_detection/readme.rst](https://github.com/bnelair/best-toolbox/blob/master/projects/slow_wave_detection/readme.rst)

## 300 **Statistics**

301 We used linear mixed-effects models (LMMs) and generalized linear mixed-effects models  
302 (GLMMs) to analyze the effect of seizures on SWA and sleep duration. All statistical  
303 analyses were conducted in R programming language. Models were fit using the “lme4”  
304 package, with adjusted means and comparisons calculated via the “emmeans” package.  
305 LMMs were fitted using restricted maximum likelihood (REML), and degrees of freedom  
306 were approximated using the Satterthwaite method. All post-hoc comparisons were adjusted  
307 using the Tukey method.

308 For models with SWA (delta power or delta slope) as the dependent variable, we included a  
309 random intercept for each patient-channel interaction to account for repeated measures  
310 within subjects and channels. For sleep duration models, which were summarized at the  
311 patient level, we included only patient as a random intercept.

312 Data were categorized using several fixed-effect predictors. These included “channel-type”,  
313 defined as SOZ versus NSOZ; “night-type”, defined as “post-ictal” (nights following a  
314 seizure) versus “inter-ictal” nights without a preceding seizure; and “night-time”, defined as  
315 “Early” (NREM within 2 hours of sleep onset) versus “Late” (NREM more than 4 hours after  
316 sleep onset).

317 For analyzing the effect of post-ictal slowing on sleep length and SWA, we defined  
318 immediate post-ictal activity as the 10-minute interval starting 1 minute after seizure offset.  
319 The control inter-ictal activity was defined 10-minute intervals starting 3 hours before sleep  
320 onset. Separate models were fitted to the NC and mT datasets. We also created a combined  
321 dataset model for the sleep duration models.

322 The analysis of sleep duration involved several LMMs. The sleep duration model included  
323 “night-type” as the sole fixed-effect predictor. In a separate model, NREM and REM  
324 durations were modeled jointly using the interaction term “night-type” \* “sleep-stage”  
325 (NREM/REM), which included separate random effects for patient for both NREM and REM.

326 To analyze the quantitative effect of seizure duration, another LMM for sleep duration used  
327 “seizure length” as its sole predictor. Additional LMMs examining the effect of seizure length  
328 on SWA power and slope included both “seizure length” and “channel-type” as predictors.  
329 Total seizure duration was calculated as the total time in seizure over the 24-hour period  
330 preceding (‘ictal day’) the analyzed post-ictal nights. Standardized beta coefficients were  
331 calculated for the seizure length estimates from these models.

332 Changes in SWA (delta power and slope) during post-ictal nights were investigated using a  
333 GLMM with a Gamma distribution and log-link function. This model's fixed effects included  
334 “channel-type”, “night-type”, and “night-time”, along with two interaction terms: “channel-  
335 type” \* “night-type” and “night-time” \* “night-type”.

336 Finally, to quantify the relationship between post-ictal power, SWA (delta power and delta  
337 slope), we performed a series of linear regressions. These fits were calculated for each

338 unique patient-channel combination and stratified by “night-type” (inter-ictal vs. post-ictal)  
339 and “channel-type” (SOZ vs. NSOZ). The strength of each linear fit was determined by the  
340 Pearson's r-value. The resulting distributions of r-values from inter-ictal and post-ictal  
341 periods were then compared separately for SOZ and NSOZ channels using a Wilcoxon rank-  
342 sum test.

## 343 **Results**

344 We analyzed two unique long-term LFP datasets from 16 participants with focal drug-  
345 resistant mesial temporal lobe epilepsy (mT) and neocortical epilepsy (NC). Our selection  
346 criteria, mainly driven by sufficient LFP data rates that allows for the analysis, were fulfilled in  
347 6/11 NC and 5/5 mT participants. A final selection of the 11 patients (5 mT and 6 NC) and  
348 their demographics is shown in Table 1. Overall, across all participants, our study analyzed a  
349 dataset including 1,501 days with 1,223 days in interictal category and 278 days in postictal  
350 category (Table 2).

351 **Table 1 and Table 2 near here.**

352 **Figure 1 near here.**

### 353 **Seizures in Ambulatory Participants with Focal Epilepsy**

354 The 11 participants had seizures originating from hippocampus (5/11), temporal neocortex  
355 (3/11), frontal neocortex (2/11), or parietal neocortex (1/11) (Table 1). The circadian-  
356 ultradian distribution of seizures varied across participants. Seizures were classified into  
357 diurnal (daytime: 8AM – 12-midnight), nocturnal (>12midnight – 8AM), or mixed. The  
358 participants with mT had mostly diurnal seizures with subject specific unimodal, bimodal or  
359 uniform distribution patterns. The participants with neocortical epilepsy have a more varied  
360 temporal distribution of seizures occurrence with both nocturnal and diurnal patterns (Figure  
361 2 A&C).

## 362 **Distribution of Sleep Stages Across Nights in Ambulatory**

### 363 **Participants with Focal Epilepsy**

364 The performance of sleep scoring classifier yielded an overall F-1 score of 0.90. Sub-epoch  
365 performance was  $F_1 = 0.94$  for REM,  $F_1 = 0.83$  for Awake, and  $F_1=0.67$  for REM sleep. This  
366 scoring methodology is consistent with prior analyses of the dataset (Mivalt et al. 2022;  
367 Kremen et al. 2025; Mivalt, Sladky, et al. 2023). Lacking gold-standard sleep annotations for  
368 the Neocortical (NC) cohort, we adapted our previously validated classification approach. To  
369 establish performance relevant to the NC channel locations, we re-trained the  
370 classifier exclusively using the neocortical channels from a combined dataset from Kremen  
371 et al (Kremen et al. 2019) (LFP recorded with iEEG strips and grids only, scalp EEG, and  
372 gold-standard PSG annotations) for each patient and then transferred the approach to the  
373 NC dataset. This yielded an overall accuracy of 0.87 and an estimated  $F_1$  score of 0.82 for  
374 Awake,  $F_1 = 0.87$  for NREM, and  $F_1=0.65$  for REM, which was deemed acceptable for  
375 transfer to the NC data. While this performance was marginally lower than the original  
376 published results that incorporated sEEG electrodes (Kremen et al. 2019), the core  
377 classification methodology for the NC data aligns with our prior work (Kremen et al. 2019;  
378 Mivalt et al. 2022; Mivalt, Sladky, et al. 2023). The same results for NC sleep classification  
379 (sleep labels) were previously used in studies analyzing the NeuroVista data (Dell et al.  
380 2021; Payne et al. 2021).

381 The circular histograms of the diurnal distribution of behavioral states (Wakefulness, NREM,  
382 REM) and seizures reveal participant-specific seizure and sleep patterns (Figure 2). Except  
383 for participants mT-2 & NC-3 who had very little REM, the circular histograms for sleep-wake  
384 show increased NREM compared to REM in the early part of the night followed by shift to  
385 more NREM/REM cycles with longer REM sleep duration later in the night, as was reported  
386 in limited duration sleep-wake studies (Merica and Gaillard 1986; Fuller, Gooley, and Saper  
387 2006). Three participants with mT had markedly reduced REM/NREM ratios (mT-2, NC-3,

388 NC-5). The remaining participants had more physiologically normal sleep distributions, with  
389 more NREM sleep early in the night and more REM sleep later in the night sleep cycle.

390 **Figure 2 near here.**

## 391 **Seizure-associated alterations in sleep architecture and** 392 **electrophysiology**

393 Analysis of sleep duration (Figure 3, Table 3, Table S1) shows the alternation of total sleep  
394 duration and NREM sleep in post-ictal versus inter-ictal sleep. Both average total sleep time  
395 (TST) and average NREM sleep time across participants were longer during nights following  
396 daytime seizures (post-ictal nights) than for interictal nights. Average postictal night TST was  
397  $8.83 \pm 0.30$  hours vs. interictal night TST of  $8.43 \pm 0.29$  hours ( $p < 0.01$ ), while post-ictal night  
398 average NREM sleep time was  $6.03 \pm 0.29$  hours vs. interictal night NREM sleep time of  
399  $5.69 \pm 0.29$  hours ( $p < 0.001$ ). On the contrary the REM phase of sleep was shortened, with  
400  $1.47 \pm 0.21$  hours post-ictal vs.  $1.67 \pm 0.20$  in interictal nights ( $p < 0.05$ , Table 3).

401 **Figure 3 and Table 3 near here.**

402

403 There were also post-ictal sleep changes on microarchitectural and electrophysiological  
404 levels. Both SWA (1 – 3 Hz power and LFP waveform slope) during NREM sleep were  
405 increased on post-ictal nights compared to inter-ictal nights (Figure 4, Table 4). The delta  
406 LFP power was higher in post-ictal sleep in both cohorts in early and late phases of the  
407 night, but larger in the early night (Table 4). Furthermore, the increased SWA (both power  
408 and slope) were greater in the SOZ compared to NSOZ in the neocortical participants where  
409 the analysis was possible (Table 4). The increased delta power was greater during the early  
410 portion of the night (first two hours of the night) but also persisted into the latter half of the  
411 night (more than 4 hours into the night) in both SOZ and NSOZ electrodes. Similar  
412 results appeared in the mT cohort during the early night, involving only the SOZ electrodes,

413 where SWA (both delta power and slope) were higher in the early part of post-ictal nights.  
414 Notably, we found similar findings of larger post-ictal effects on SWA early in the night  
415 compared to later in the sleep cycle, consistent with previous observations from shorter data  
416 sets by Boly et al. (Boly et al. 2017).

417 **Figure 4 and Table 4 near here.**

418 We also investigated if there were any effects of seizure length (distributions of seizure  
419 durations for each patient is shown in supplementary data in Figure S4) or  
420 electrophysiological post-ictal slowing on electrophysiology dynamics of SWA and sleep  
421 structure at nights after seizures. Our results suggest that seizure duration calculated as a  
422 sum of the durations of all seizures occurring during the ictal day preceding the analyzed  
423 post-ictal night does not significantly affect total sleep, NREM, or REM duration and has  
424 minimal impact on SWA (both delta power and slope) in early phase of post-ictal nights  
425 (Figure 5 and Table 5). To test the effect of post-ictal slowing on SWA in post-ictal nights,  
426 we characterized post-ictal slowing as a post-ictal delta power and tested its effect on SWA  
427 electrophysiological markers (delta power and slope). We found that post-ictal delta power is  
428 less correlated with SWA (delta power and slope) than during control interictal days. The  
429 median r-value = 0.26 for delta power in post-ictal nights while in inter-ictal night median r-  
430 value = 0.56 ( $p < 0.01$ ). Similarly for delta slope median r-value in post-ictal nights is 0.24  
431 compared to 0.49 in inter-ictal nights ( $p < 0.001$ ). This was only true in pathological regions of  
432 the brain in SOZ electrodes while there was no effect found in NSOZ electrodes (Figure 6).

433 **Figure 5 and 6 near here.**

## 434 **Discussion**

435 This study investigated post-ictal slow wave sleep using long-term continuous LFP  
436 recordings in ambulatory participants with focal epilepsy living in their natural home  
437 environment. We quantified inter-ictal and post-ictal slow-wave sleep and observed

438 consistent changes in post-ictal slow wave sleep duration, SWA spectral power, and SWA  
439 slope. While increased NREM sleep duration may simply reflect the brain's restorative  
440 process following the physiological stress of a seizure, our electrophysiological findings are  
441 consistent with studies of systems-related consolidation with enhanced slow-wave activity as  
442 a key biomarker (Klinzing, Niethard, and Born 2019). Similar findings were also reported in  
443 short-term scalp EEG studies where sleep SWA power and waveform slope were positively  
444 correlated with the frequency of secondary generalized seizures in the days preceding sleep  
445 and at scalp locations associated with the underlying focal epilepsy localization (Boly et al.  
446 2017; Moffet et al. 2020). Focal increases in sleep SWA in the nights after motor learning  
447 tasks have also been described in neurologically normal research participants (Huber et al.  
448 2004). In summary, the findings presented here support a process of seizure-related  
449 consolidation in human focal epilepsy. While prior studies of systems-related consolidation  
450 have largely focused on NREM sleep, and where we report consistent electrophysiology  
451 features, the exploration of post-ictal REM sleep changes is relevant for a complete picture  
452 of memory and emotional regulation. Here we found that overall REM sleep duration is  
453 decreased in the nights after seizures. This is consistent with previously reported findings in  
454 short-term studies at Epilepsy Monitoring Units (Bazil, Castro, and Walczak 2000; Nobili et  
455 al. 2025). Future investigations will focus more broadly on focal epilepsy sleep architecture.

456

457 Furthermore, animal models support targeting consolidation to disrupt seizure related  
458 consolidation in epileptic networks (Lai et al. 2024; Ferrero et al. 2025). Lai et al. recently  
459 showed that a mammalian target of rapamycin (mTOR) signaling pathway inhibitor delivered  
460 during the post-ictal period yielded the largest seizure and IES reduction, and subsequently  
461 demonstrated similar findings for IES in a pilot human trial. While Ferrero et al. showed how  
462 properly spatiotemporally targeted closed-loop electrical brain stimulation can eliminate the  
463 abnormal cortical activity patterns and prevent progression of long-term spatial memory

464 deficits in rodents with epilepsy. These studies suggest the potential importance of post-ictal  
465 targeting of interventions to prevent or reduce pathologic consolidation of epilepsy engrams.

466

467 Studies in larger numbers of participants are required to confirm the preliminary findings  
468 reported here. Future studies should also address the relationships between sleep patterns  
469 and common comorbidities, such as memory, mood and cognitive dysfunction. Lastly, these  
470 findings may prove useful for investigating targeted neuromodulation using currently  
471 available brain stimulation devices to disrupt consolidation of seizure engrams during post-  
472 ictal slow wave sleep. We have recently initiated such a trial in people with focal epilepsy  
473 implanted with anterior nucleus of thalamus FDA approved devices.

## 474 **Data and Software Availability**

475 The data underlying this article will be shared upon reasonable request to the corresponding  
476 authors. The software tools created by authors and used for this article are published at  
477 Mayo Clinic's Bioelectronics Neurophysiology and Engineering Laboratory webpage  
478 (<https://www.mayo.edu/research/labs/bioelectronics-neurophysiology-engineering/overview>)  
479 and Github repository (<https://github.com/bnelair>).

## 480 **References**

- 481 Bazil, Carl W. 2017. "Sleep and Epilepsy." *Seminars in Neurology* 37 (4): 407–12.
- 482 Bazil, Carl W., Luiz H. M. Castro, and Thaddeus S. Walczak. 2000. "Reduction of Rapid Eye  
483 Movement Sleep by Diurnal and Nocturnal Seizures in Temporal Lobe Epilepsy."  
484 *Archives of Neurology* 57 (3): 363.
- 485 Bersagliere, Alessia, and Peter Achermann. 2010. "Slow Oscillations in Human Non-Rapid  
486 Eye Movement Sleep Electroencephalogram: Effects of Increased Sleep Pressure."  
487 *Journal of Sleep Research* 19 (1 Pt 2): 228–37.

- 488 Boly, Melanie, Benjamin Jones, Graham Findlay, Erin Plumley, Armand Mensen, Bruce  
489 Hermann, Guilio Tononi, and Rama Maganti. 2017. "Altered Sleep Homeostasis  
490 Correlates with Cognitive Impairment in Patients with Focal Epilepsy." *Brain: A*  
491 *Journal of Neurology*. <https://doi.org/10.1093/brain/awx017>.
- 492 Bower, Mark R. 2024. "Review: Seizure-Related Consolidation and the Network Theory of  
493 Epilepsy." *Frontiers in Network Physiology* 4 (August): 1430934.
- 494 Bower, Mark R., Michal T. Kucewicz, Erik K. St. Louis, Fredric B. Meyer, W. Richard Marsh,  
495 Matt Stead, and Gregory A. Worrell. 2017. "Reactivation of Seizure-Related Changes  
496 to Interictal Spike Shape and Synchrony during Postseizure Sleep in Patients."  
497 *Epilepsia* 58 (1): 94–104.
- 498 Bower, Mark, M. Stead, R. S. Bower, M. T. Kucewicz, V. Sulc, J. Cimbalnik, B. H.  
499 Brinkmann, et al. 2015. "Evidence for Consolidation of Neuronal Assemblies after  
500 Seizures in Humans." *Journal of Neuroscience* 35 (3).  
501 <https://doi.org/10.1523/JNEUROSCI.3019-14.2015>.
- 502 Carvalho, Diego Z., Vaclav Kremen, Filip Mivalt, Erik K. St Louis, Stuart J. McCarter, Jan  
503 Bukartyk, Scott A. Przybelski, et al. 2024. "Non-Rapid Eye Movement Sleep Slow-  
504 Wave Activity Features Are Associated with Amyloid Accumulation in Older Adults  
505 with Obstructive Sleep Apnoea." *Brain Communications* 6 (5): fcae354.
- 506 Cook, Mark J., Terence J. O'Brien, Samuel F. Berkovic, Michael Murphy, Andrew Morokoff,  
507 Gavin Fabinyi, Wendyl D'Souza, et al. 2013. "Prediction of Seizure Likelihood with a  
508 Long-Term, Implanted Seizure Advisory System in Patients with Drug-Resistant  
509 Epilepsy: A First-in-Man Study." *Lancet Neurology* 12 (6): 563–71.
- 510 Dell, Katrina L., Daniel E. Payne, Vaclav Kremen, Matias I. Maturana, Vaclav Gerla, Petr  
511 Nejedly, Gregory A. Worrell, et al. 2021. "Seizure Likelihood Varies with Day-to-Day  
512 Variations in Sleep Duration in Patients with Refractory Focal Epilepsy: A  
513 Longitudinal Electroencephalography Investigation." *EClinicalMedicine* 37 (July).  
514 <https://doi.org/10.1016/j.eclinm.2021.100934>.
- 515 Diekelmann, Susanne, and Jan Born. 2010. "The Memory Function of Sleep." *Nature*  
516 *Reviews. Neuroscience* 11 (2): 114–26.
- 517 Elger, Christian E., and Christian Hoppe. 2018. "Diagnostic Challenges in Epilepsy: Seizure  
518 under-Reporting and Seizure Detection." *Lancet Neurology* 17 (3): 279–88.
- 519 Ferrero, Jose J., Ahnaf R. Hassan, Zelin Yu, Zifang Zhao, Liang Ma, Cynthia Wu, Shan  
520 Shao, et al. 2025. "Closed-Loop Electrical Stimulation Prevents Focal Epilepsy  
521 Progression and Long-Term Memory Impairment." *Nature Neuroscience* 28 (8):  
522 1753–62.
- 523 Fuller, Patrick M., Joshua J. Gooley, and Clifford B. Saper. 2006. "Neurobiology of the  
524 Sleep-Wake Cycle: Sleep Architecture, Circadian Regulation, and Regulatory  
525 Feedback." *Journal of Biological Rhythms* 21 (6): 482–93.
- 526 Goddard, G. V., and R. M. Douglas. 1975. "Does the Engram of Kindling Model the Engram  
527 of Normal Long Term Memory?" *The Canadian Journal of Neurological Sciences. Le*  
528 *Journal Canadien Des Sciences Neurologiques* 2 (4): 385–94.

- 529 Gowers, W. R. 1885. "Recent Literature Lectures on the Diagnosis of Diseases of the Brain,  
530 Delivered at University College Hospital." *The Boston Medical and Surgical Journal*  
531 113 (26): 624–25.
- 532 Hermann, Bruce, Lisa L. Conant, Cole J. Cook, Gyujoon Hwang, Camille Garcia-Ramos,  
533 Kevin Dabbs, Veena A. Nair, et al. 2020. "Network, Clinical and Sociodemographic  
534 Features of Cognitive Phenotypes in Temporal Lobe Epilepsy." *NeuroImage. Clinical*  
535 27 (102341): 102341.
- 536 Hsu, David, Wei Chen, Murielle Hsu, and John M. Beggs. 2008. "An Open Hypothesis: Is  
537 Epilepsy Learned, and Can It Be Unlearned?" *Epilepsy and Behavior*.  
538 <https://doi.org/10.1016/j.yebeh.2008.05.007>.
- 539 Huber, Reto, M. Felice Ghilardi, Marcello Massimini, and Giulio Tononi. 2004. "Local Sleep  
540 and Learning." *Nature*. <https://doi.org/10.1038/nature02663>.
- 541 Jaramillo, V., C. Volk, A. Maric, M. Furrer, S. Fattinger, S. Kurth, C. Lustenberger, and R.  
542 Huber. 2020. "Characterization of Overnight Slow-Wave Slope Changes across  
543 Development in an Age-, Amplitude-, and Region-Dependent Manner." *Sleep* 43 (9).  
544 <https://doi.org/10.1093/sleep/zsaa038>.
- 545 Klinzing, Jens G., Niels Niethard, and Jan Born. 2019. "Mechanisms of Systems Memory  
546 Consolidation during Sleep." *Nature Neuroscience* 22 (10): 1598–1610.
- 547 Kremen, B. H. Brinkmann, J. J. Van Gompel, M. Stead, E. K. St Louis, and G. A. Worrell.  
548 2019. "Automated Unsupervised Behavioral State Classification Using Intracranial  
549 Electrophysiology." *Journal of Neural Engineering* 16 (2).  
550 <https://doi.org/10.1088/1741-2552/aae5ab>.
- 551 Kremen, J. J. Duque, B. H. Brinkmann, B. M. Berry, M. T. Kucewicz, F. Khadjevand, J. Van  
552 Gompel, M. Stead, E. K. St Louis, and G. A. Worrell. 2017. "Behavioral State  
553 Classification in Epileptic Brain Using Intracranial Electrophysiology." *Journal of*  
554 *Neural Engineering* 14 (2). <https://doi.org/10.1088/1741-2552/aa5688>.
- 555 Kremen, Vaclav, Vladimir Sladky, Filip Mivalt, Nicholas M. Gregg, Irena M. Balzekas, Tory  
556 Marks, Benjamin Henry Brinkmann, et al. 2024. "Platform for Brain Network Sensing  
557 and Stimulation with Quantitative Behavioral Tracking: Application to Limbic Circuit  
558 Epilepsy." medRxiv. <https://doi.org/10.1101/2024.02.09.24302358>.
- 559 Kremen, Vaclav, Vladimir Sladky, Filip Mivalt, Nicholas M. Gregg, Benjamin H. Brinkmann,  
560 Irena Balzekas, Victoria Marks, et al. 2025. "Modulating Limbic Circuits in Temporal  
561 Lobe Epilepsy: Impacts on Seizures, Memory, Mood and Sleep." *Brain*  
562 *Communications* 7 (2): fcaf106.
- 563 Lai, Shirong, Libo Zhang, Xinyu Tu, Xinyue Ma, Yujing Song, Kexin Cao, Miaomiao Li, et al.  
564 2024. "Termination of Convulsion Seizures by Destabilizing and Perturbing Seizure  
565 Memory Engrams." *Science Advances* 10 (12): eadk9484.
- 566 Lauderdale, Diane S., Kristen L. Knutson, Lijing L. Yan, Kiang Liu, and Paul J. Rathouz.  
567 2008. "Self-Reported and Measured Sleep Duration: How Similar Are They?"  
568 *Epidemiology (Cambridge, Mass.)* 19 (6): 838–45.

- 569 Marshall, Lisa, Halla Helgadóttir, Matthias Mölle, and Jan Born. 2006. "Boosting Slow  
570 Oscillations during Sleep Potentiates Memory." *Nature* 444 (7119): 610–13.
- 571 Merica, H., and J-M Gaillard. 1986. "Internal Structure of Sleep Cycles in a Healthy  
572 Population." *Sleep* 9 (4): 502–13.
- 573 Mivalt, Filip, Vaclav Kremen, Vladimir Sladky, Irena Balzekas, Petr Nejedly, Nicholas M.  
574 Gregg, Brian Nils Lundstrom, et al. 2022. "Electrical Brain Stimulation and  
575 Continuous Behavioral State Tracking in Ambulatory Humans." *Journal of Neural  
576 Engineering* 19 (1): 016019.
- 577 Mivalt, Filip, Vaclav Kremen, Vladimir Sladky, Jie Cui, Nicholas M. Gregg, Irena Balzekas,  
578 Victoria Marks, et al. 2023. "Impedance Rhythms in Human Limbic System." *Journal  
579 of Neuroscience* 43 (39): 6653–66.
- 580 Mivalt, Filip, Vladimir Sladky, Samuel Worrell, Nicholas M. Gregg, Irena Balzekas, Inyong  
581 Kim, Su-Youne Chang, et al. 2023. "Automated Sleep Classification with Chronic  
582 Neural Implants in Freely Behaving Canines." *Journal of Neural Engineering* 20 (4):  
583 046025.
- 584 Moffet, Eric W., Ruben Verhagen, Benjamin Jones, Graham Findlay, Elsa Juan, Tom  
585 Bugnon, Armand Mensen, et al. 2020. "Local Sleep Slow-Wave Activity Colocalizes  
586 With the Ictal Symptomatogenic Zone in a Patient With Reflex Epilepsy: A High-  
587 Density EEG Study." *Frontiers in Systems Neuroscience*.  
588 <https://doi.org/10.3389/fnsys.2020.549309>.
- 589 Nejedly, Petr, Vaclav Kremen, Vladimir Sladky, Mona Nasser, Hari Guragain, Petr Klimes,  
590 Jan Cimbalnik, Yogatheesan Varatharajah, Benjamin H. Brinkmann, and Gregory A.  
591 Worrell. 2019. "Deep-Learning for Seizure Forecasting in Canines with Epilepsy."  
592 *Journal of Neural Engineering* 16 (3): 036031.
- 593 Nobili, Lino, Ramona Cordani, Dario Arnaldi, Pietro Mattioli, Marco Veneruso, and Marcus  
594 Ng. 2025. "Rapid Eye Movement Sleep and Epilepsy: Exploring Interactions and  
595 Therapeutic Prospects." *Journal of Sleep Research* 34 (2): e14251.
- 596 Payne, Daniel E., Katrina L. Dell, Phillipa J. Karoly, Vaclav Kremen, Vaclav Gerla, Levin  
597 Kuhlmann, Gregory A. Worrell, Mark J. Cook, David B. Grayden, and Dean R.  
598 Freestone. 2021. "Identifying Seizure Risk Factors: A Comparison of Sleep, Weather,  
599 and Temporal Features Using a Bayesian Forecast." *Epilepsia* 62 (2): 371–82.
- 600 Peter-Derex, Laure, Petr Klimes, Véronique Latreille, Sarah Bouhadoun, François Dubeau,  
601 and Birgit Frauscher. 2020. "Sleep Disruption in Epilepsy: Ictal and Interictal Epileptic  
602 Activity Matter." *Annals of Neurology* 88 (5): 907–20.
- 603 Riedner, Brady a., Vladyslav V. Vyazovskiy, Reto Huber, Marcello Massimini, Steve Esser,  
604 Michael Murphy, and Giulio Tononi. 2007. "Sleep Homeostasis and Cortical  
605 Synchronization: III. A High-Density EEG Study of Sleep Slow Waves in Humans."  
606 *Sleep* 30 (12): 1643–57.
- 607 Silber, Michael H. 2012. "Staging Sleep." *Sleep Medicine Clinics* 7 (3): 487–96.
- 608 Sladky, Vladimir, Petr Nejedly, Filip Mivalt, Benjamin H. Brinkmann, Inyong Kim, Erik K. St.  
609 Louis, Nicholas M. Gregg, et al. 2022. "Distributed Brain Co-Processor for Tracking

610 Spikes, Seizures and Behaviour during Electrical Brain Stimulation." *Brain*  
611 *Communications* 4 (3): fcac115.

612 Varga, Andrew W., Margaret E. Wohlleber, Sandra Giménez, Sergio Romero, Joan F.  
613 Alonso, Emma L. Ducca, Korey Kam, et al. 2016. "Reduced Slow-Wave Sleep Is  
614 Associated with High Cerebrospinal Fluid A $\beta$ 42 Levels in Cognitively Normal Elderly."  
615 *Sleep* 39 (11): 2041–48.

616 Walker, Matthew P., and Robert Stickgold. 2010. "Overnight Alchemy: Sleep-Dependent  
617 Memory Evolution." *Nature Reviews. Neuroscience*. Springer Science and Business  
618 Media LLC.

619 Zheng, Neil S., Jeffrey Annis, Hiral Master, Lide Han, Karla Gleichauf, Jack H. Ching,  
620 Melody Nasser, et al. 2024. "Sleep Patterns and Risk of Chronic Disease as  
621 Measured by Long-Term Monitoring with Commercial Wearable Devices in the All of  
622 Us Research Program." *Nature Medicine* 30 (9): 2648–56.

623

JNeurosci Accepted Manuscript

## 624 **Figure legends**

625

626 **Figure 1. Continuous long-term monitoring of local field potentials (LFP) in people**  
627 **with drug resistant focal epilepsy. (A)** Investigational implantable neural sensing devices  
628 were used to record continuous long-term LFP from amygdala-hippocampus in 5 participants  
629 with mesial temporal lobe epilepsy (mT) and in 6 participants with frontal, temporal or  
630 parietal neocortical epilepsy. **(B)** Validated automated machine learning algorithms were  
631 used to detect electrographic seizures and to classify each 10 second window of continuous  
632 LFP as inter-ictal (non-seizure) or ictal (seizure). **(C)** Sleep-wake state was classified as  
633 wakefulness (W), rapid eye movement (REM) or REM (N1, N2, or N3) sleep. **(D)** The data  
634 were split into nights after seizures (post-ictal) and nights without prior seizures in last 48-  
635 hours (inter-ictal). The duration of wakefulness, NREM, and REM and slow-wave sleep  
636 activity LFP micro-sleep features were analyzed.

637

638

639 **Figure 2. Circadian distributions of seizures and sleep-wake using continuous long-**  
640 **term local field potentials (LFP).** The LFP recorded from participants with mesial temporal  
641 epilepsy (mT) or neocortical focal epilepsy (NC) over months. **(A)** 5 participants with mT  
642 (mT 1-5) and seizures recorded from amygdala-hippocampus. Seizures were diurnal with  
643 seizures occurring at participant specific time-of-day. **(B)** Participants with focal neocortical  
644 seizures recorded from temporal (NC 1-3), frontal (NC 4-5) and parietal (NC-6) localizations.  
645 One participant had nocturnal seizures (NC-3) with decreased REM during the night **(C&D)**  
646 Circular histograms of sleep-wake states for mT and NC participants (frontal, temporal and  
647 parietal).

648

649 **Figure 3. Macro-architecture of inter-ictal and post-ictal sleep.** Total sleep duration is  
650 the is the elapsed time from sleep onset to sleep offset. NREM sleep duration is the sum of  
651 all NREM sleep stages. Total sleep time duration as well as NREM duration was increased  
652 for post-ictal versus inter-ictal slow-wave sleep. REM sleep duration, however was shorter  
653 on nights after seizures compared to inter-ictal nights. Individual subject mean values  $\pm$   
654 standard deviation in gray. The Black lines represent estimated fixed effects of a Linear  
655 Mixed Effect Model (\*  $p < 0.05$ , \*\*  $p < 0.01$ , \*\*\*\*  $p < 0.0001$ ) with error bars showing 95%  
656 confidence intervals.

657

658 **Figure 4. Micro-architecture of sleep in post-ictal nights.** Analysis of Local field  
659 potentials (LFP) in slow-wave (NREM) sleep in inter-ictal nights and post-ictal nights after  
660 seizures. Inter-ictal night was defined by absence of seizures during the preceding **24** hours.  
661 Post-ictal night was defined as sleep after seizures during awake time preceding the night.  
662 The LFP slow-wave analysis during NREM sleep was performed to quantify the slow-wave  
663 slope (**Top**) and delta frequency (1 - 3 Hz) band power (**Bottom**). The LFP slow-wave slope  
664 was increased during post-ictal nights compared to inter-ictal nights for both mT and NC  
665 participants. The LFP delta power was increased during post-ictal nights compared to inter-  
666 ictal nights for mT and NC participants. Same trend is visible in both seizure onset zone  
667 (SOZ) and non-seizure onset zone (NSOZ) electrodes. For both, delta band power and delta  
668 slope the absolute values are higher at SOZ versus NSOZ electrodes. In NC cohort, SOZ  
669 electrodes have a positive significant interaction in postictal nights for Delta power ( $p < 0.05$ ),  
670 and Delta slope ( $p < 0.01$ ). The results show Estimated Marginal Means (EMMs) contrasts  
671 from the output of Generalized Linear Mixed Effect Model. Error bars represent 95%  
672 confidence intervals. P-values were adjusted for multiple comparisons using the Tukey  
673 method. (\*  $p < 0.05$ , \*\*\*\*  $p < 0.0001$ ).

674

675

676

677 **Figure 5. Effect of seizure length on electrophysiological biomarkers in post-ictal**  
678 **nights.** The figure shows distribution of a logarithmic Delta power and Slope and seizure  
679 length across NC dataset in early post-ictal nights (first two hours). The lines are the fitted  
680 coefficients of Linear Mixed Effect Model (LMM) with shaded area representing 95%  
681 confidence intervals. The data points are corrected by removing the patient/channel-specific  
682 baseline variability (LMM random effect). Seizure length has similar but very minimal  
683 significant effect on Delta power (A) and Delta slope (B) in both SOZ and NSOZ channels  
684 ( $p < 0.01$ , LMM).

685

686 **Figure 6. Correlation of Postictal Power with SWA Power and SWA Slope.** The top  
687 panel shows the distribution of Pearson's r-values from linear fits between postictal power  
688 and SWA Power. The bottom panel shows the same for fits between postictal power and  
689 SWA Slope. Each data point represents a unique correlation from an individual patient-  
690 channel combination; different symbols mark patient identity. In SOZ electrodes, the  
691 correlation during postictal nights is significantly weaker and more variable compared to  
692 interictal nights (SWA Power:  $p < 0.01$ ; SWA Slope:  $p < 0.001$ ; Wilcoxon rank-sum test).

693

## Tables

Subject	Age (yrs)	Sex	Onset (yrs)	ASM	SOZ	#Days/#Seizures
<b>Seizure Advisory System (NeuroVista Inc.)</b>						
NC-1	35-40	M	5-10	CBZ, LCM, PRP, TPM	nTL; prior ATLE	465/101
NC-2	45-55	M	15-20	CBZ, CLZ, LEV, LCM	nTL, prior ATLE	534/769
NC-3	40-45	M	20-25	LTG, LCM, PHT, RTG	nTL	709/40
NC-4	50-55	F	15-20	LEV, OXC, ZNS	FT	318/897
NC-5	45-50	M	20-25	CBZ, LEV	FT	355/732
NC-6	40-45	M	10-15	LCM, LTG, OXC, VPA	OP	607/45
<b>RC+S™ (Medtronic Plc.)</b>						
mT-1	55-60	F	5-10	GBP, TZP, LGT	mTL	831/542
mT-2	20-25	F	5-10	LCM, CZP,	mTL; prior ATLE	392/15
mT-3	35-40	F	0-5	OXC, LEV	mTL	300/250
mT-4	40-45	F	30-35	CZP, LEV, CNB	mTL	401/59
mT-5	30-35	M	20-25	VPA, LCM	mTL	325/219

695

696 **Table 1. Subject Demographics.** Abbreviations: ASM = Anti-seizure medications,  
 697 CBZ=carbamazepine, CLZ=clobazam, CZP=clonazepam, LCM = lacosamide,  
 698 LEV=levetiracetam, LTG=lamotrigine, OXC=oxcarbazepine, PHT = phenytoin,  
 699 RTG=retigabine, ZNS=zonisamide, SOZ = Seizure onset zone Seizure onset zones: mTL –  
 700 mesial temporal lobe, nFT – neocortical frontotemporal, nOP – neocortical occipitoparietal,  
 701 nPT – neocortical parietal-temporal, nTL – neocortical temporal lobe.

702

703

704

705

Participant	Category	Number of days	Average dropout rate during sleep [%]	Average sleep duration [H]	Mean seizure hour during 24-hour day cycle	Circular variance
NC-1	interictal	267	0.03 ± 0.05	8.29 ± 0.98	16.0	0.61
	postictal	51	0.04 ± 0.05	8.61 ± 1.34		
NC-2	interictal	46	0.11 ± 0.06	8.52 ± 2.04	10.9	0.69

	postictal	26	0.12 ± 0.05	8.87 ± 1.59		
NC-3	interictal	549	0.02 ± 0.03	8.51 ± 2.06	12.7	0.6
	postictal	14	0.01 ± 0.02	8.57 ± 2.65		
NC-4	interictal	43	0.01 ± 0.02	8.43 ± 1.77	2.0	0.72
	postictal	42	0.02 ± 0.03	9.54 ± 1.55		
NC-5	interictal	17	0.00 ± 0.01	9.69 ± 1.31	11.5	0.74
	postictal	118	0.01 ± 0.02	9.53 ± 0.83		
NC-6	interictal	260	0.10 ± 0.06	6.43 ± 1.36	15.1	0.59
	postictal	11	0.09 ± 0.08	6.92 ± 2.08		
mT-1	interictal	7	0.07 ± 0.04	8.37 ± 1.47	17.9	0.62
	postictal	8	0.06 ± 0.05	9.09 ± 1.10		
mT-2	interictal	9	0.13 ± 0.04	8.25 ± 3.92	19.2	0.28
mT-3	interictal	8	0.07 ± 0.03	9.07 ± 0.63	15.6	0.7
	postictal	6	0.07 ± 0.03	9.51 ± 0.48		
mT-4	interictal	13	0.07 ± 0.02	9.81 ± 0.83	14.4	0.43
	postictal	1	0.07	9.70		
mT-5	interictal	4	0.12 ± 0.02	7.28 ± 1.62	12.0	0.64
	postictal	1	-	-		
<b>Total</b>	<b>interictal</b>	<b>1223</b>				
<b>Total</b>	<b>postictal</b>	<b>278</b>				

706

707

708 **Table 2. Nights included in analysis.** Total number of analyzed nights in both categories  
709 (interictal and postictal) included in analysis for each participant. This includes number of  
710 nights taken into the analysis as well as average drop-out of the data, sleep duration, and  
711 average seizure hour of the day with its circular variance for each patient and the category.

712

713

714

	mT + NC			
	Interictal	Post-Ictal	p-value	Cohen's d
Total Sleep	8.43 ± 0.29	8.83 ± 0.30	0.007	-0.24
NREM	5.69 ± 0.29	6.03 ± 0.29	0.000	-0.34
REM	1.67 ± 0.20	1.47 ± 0.21	0.020	0.20

715

716 **Table 3. Changes in postictal sleep length.** Using combined data from both cohorts, a  
717 postictal sleep is longer for about ~24 minutes than interictal sleep ( $p < 0.01$ ). The NREM  
718 sleep is longer for about ~21 minutes on average in nights after seizures compare to  
719 interictal nights ( $p < 0.001$ ), while the REM sleep is about ~12 minutes on average shorter  
720 ( $p < 0.05$ ). P-values and Cohen's d were calculated using a Linear Mixed Model (LMM).

721

722

723

JNeurosci Accepted Manuscript

724

725

		Early Night				Late Night				
		Delta	Interictal	Post-ictal	ratio	p	Interictal	Post-ictal	ratio	p
NC	NSOZ	Power $\mu\text{V}^2/\text{Hz}$	184 $\pm$ 23	219 $\pm$ 28	0.84	0.000	160 $\pm$ 20	174 $\pm$ 22	0.92	0.000
	SOZ		346 $\pm$ 40	427 $\pm$ 50	0.81	0.000	301 $\pm$ 35	339 $\pm$ 39	0.89	0.000
	NSOZ	Slope $\mu\text{V}/\text{sec}$	272 $\pm$ 15	299 $\pm$ 16	0.91	0.000	261 $\pm$ 14	271 $\pm$ 15	0.96	0.000
	SOZ		366 $\pm$ 18	412 $\pm$ 20	0.89	0.000	352 $\pm$ 17	374 $\pm$ 19	0.94	0.000
mT	SOZ	Power $\mu\text{V}^2/\text{Hz}$	1461 $\pm$ 437	1528 $\pm$ 458	0.96	0.028	1113 $\pm$ 333	1137 $\pm$ 340	0.98	0.161
	SOZ	Slope $\mu\text{V}/\text{sec}$	850 $\pm$ 160	911 $\pm$ 171	0.93	0.000	727 $\pm$ 137	741 $\pm$ 139	0.98	0.037

726

727 **Table 4. Changes in Delta band activity during interictal vs postictal nights.**728 The values are Estimated Marginal Means (EMM)  $\pm$  standard error for Delta power ( $\mu\text{V}^2/\text{Hz}$ )729 and Delta slope ( $\mu\text{V}/\text{s}$ ) within the Seizure Onset Zone (SOZ) and Non-Seizure Onset Zone

730 (NSOZ) electrodes, stratified by night period (Early vs. Late). Comparisons are made

731 between interictal nights (without any seizure the same day) and postictal nights (nights after

732 a seizure). The 'ratio' columns represent the interictal EMM divided by the postictal EMM. P-

733 values were calculated from a General Linear Mixed Model (GLMM) using a Gamma

734 distribution with a log-link function. In the NC cohort, this model also revealed a positive

735 significant interaction for SOZ electrodes in postictal nights for Delta power ( $p < 0.05$ ) and736 Delta slope ( $p < 0.01$ ). Reported p-values reflect post-hoc pairwise comparisons between the

737 interictal and postictal states, adjusted using the Tukey method.

738

739

740

	Delta power	Delta slope	Sleep duration	NREM duration	REM duration
Estimated Coefficient	0.00034	0.07019	0.00125	0.00057	0.00026
Standardized Coefficient ( $\beta$ ) [95% CI]	0.04 [0.01-0.06]	0.05 [0.02-0.08]	-	-	-
p-value	<0.01	<0.001	n.s.	n.s.	n.s.

741

742

743

744

745

746

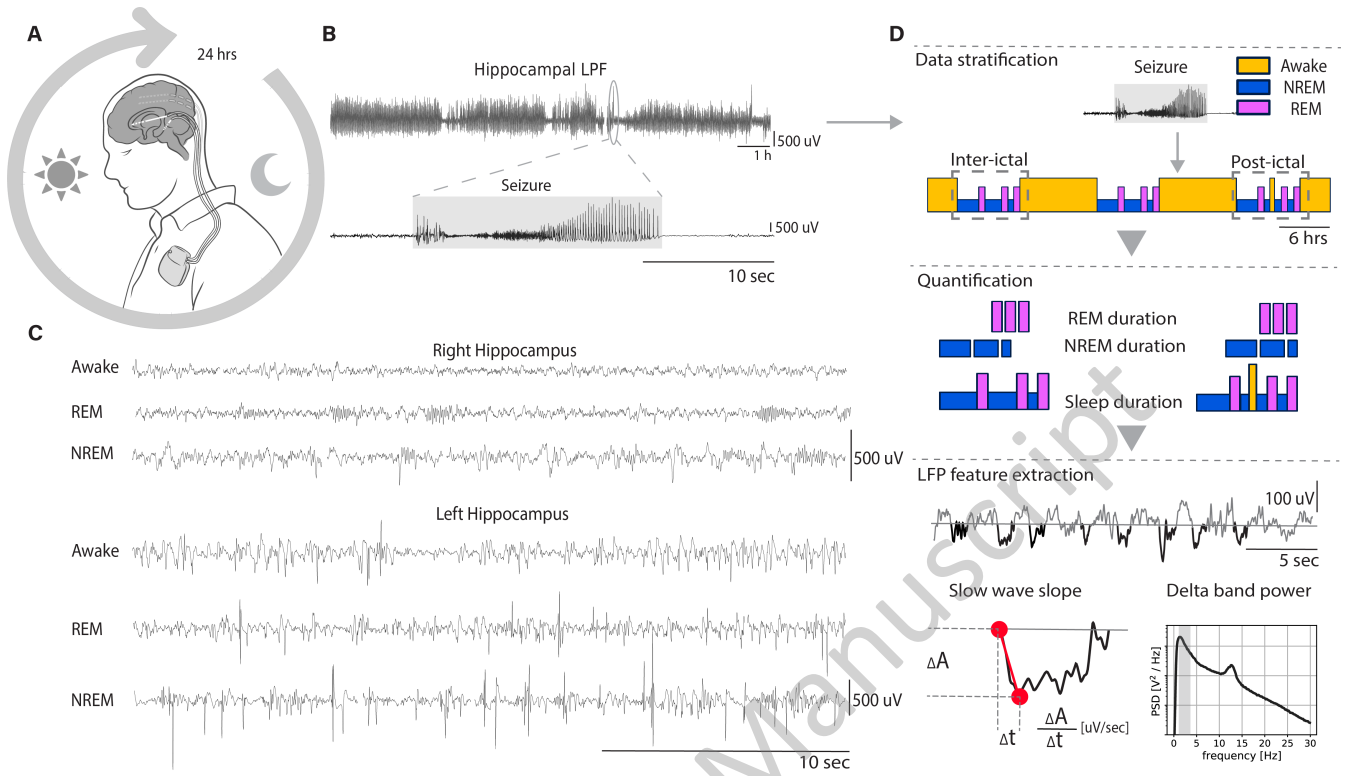
747

748

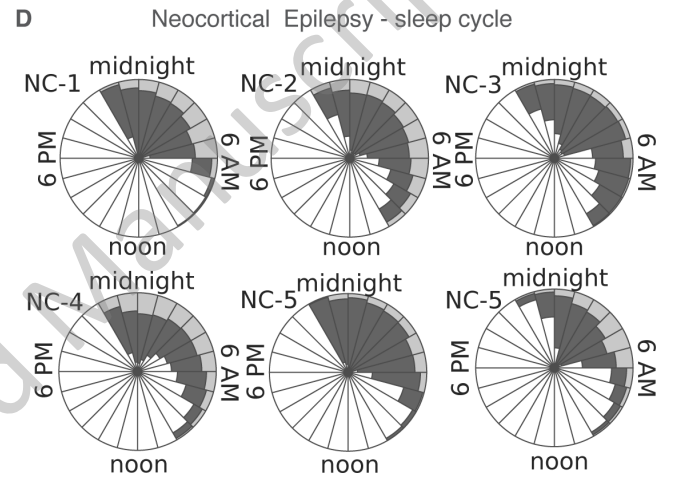
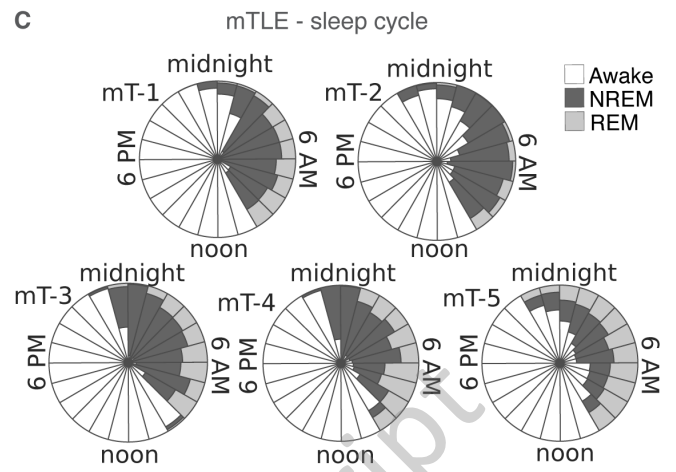
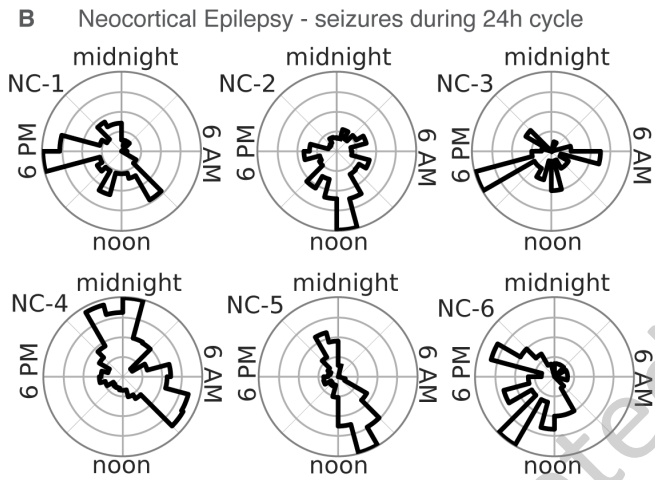
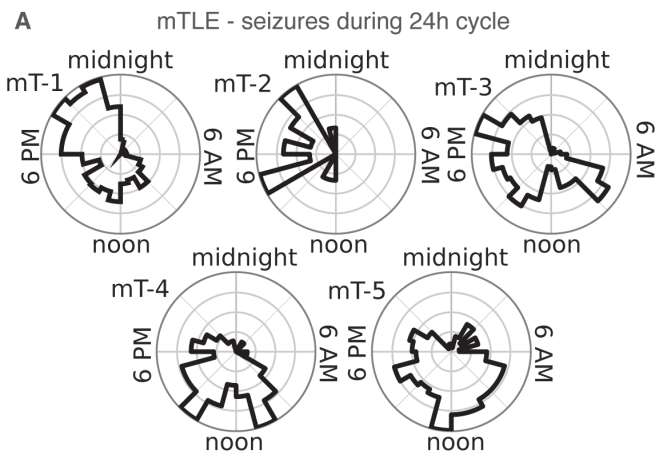
**Table 5. Effect of seizure length on sleep duration and slow-wave dynamics in NC**

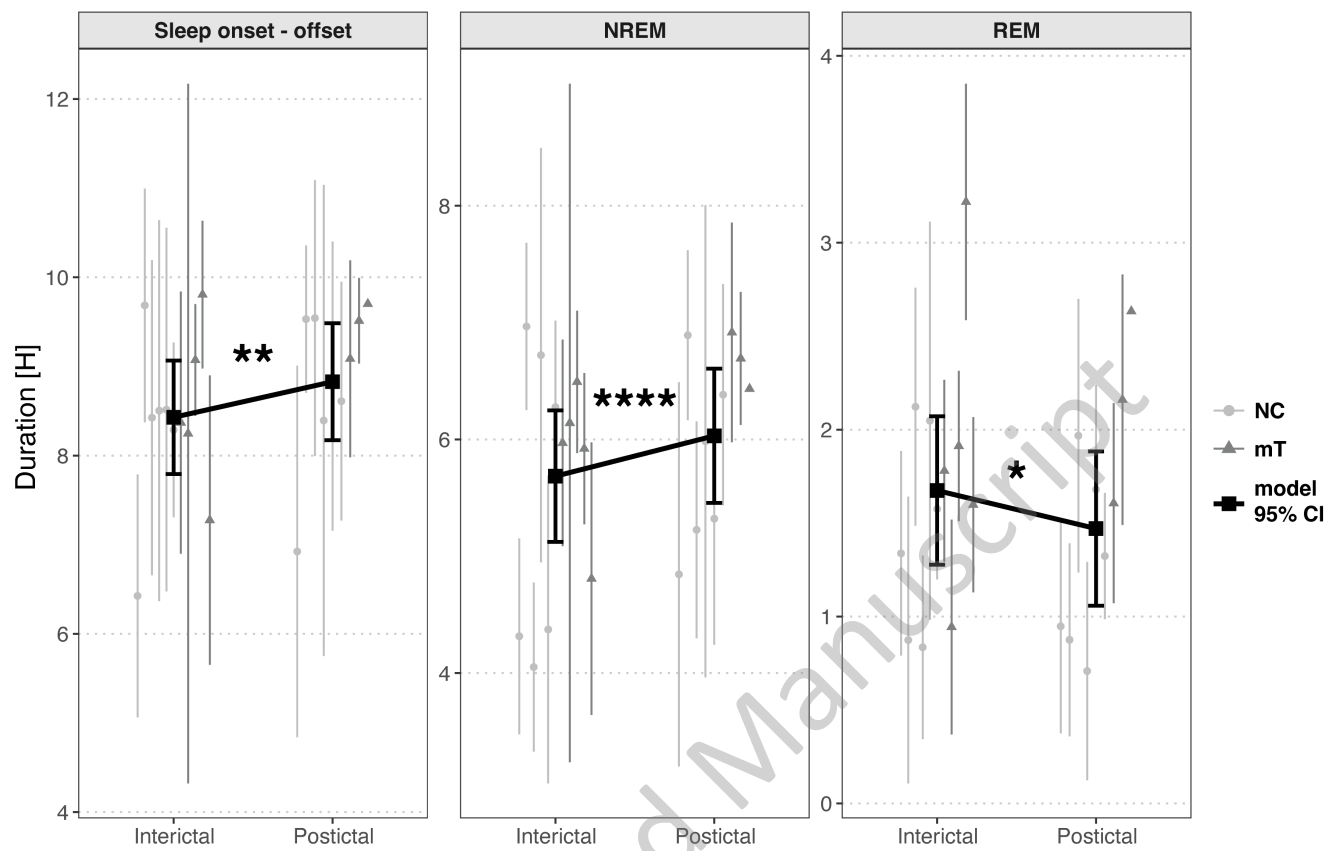
**cohort.** Results from a Linear Mixed Model (LMM) assessing the effect of seizure length on postictal Delta power, Delta slope, and sleep stage durations. The LMM shows a minimal effect size for seizure length on electrophysiological markers (Delta power and slope) and a non-significant effect on total sleep, NREM, and REM sleep durations.

JNeurosci Accepted Manuscript

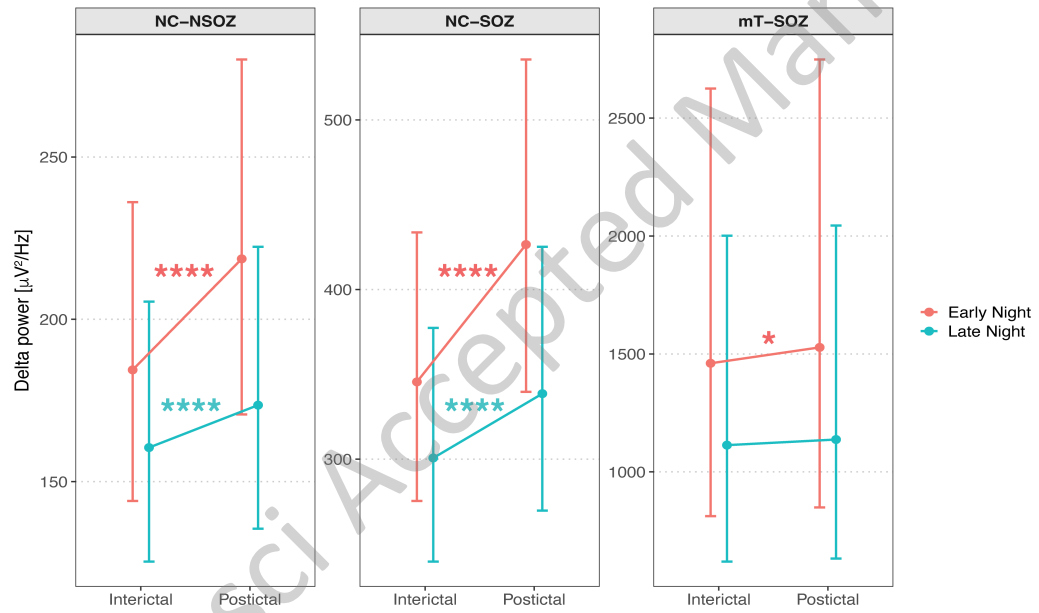
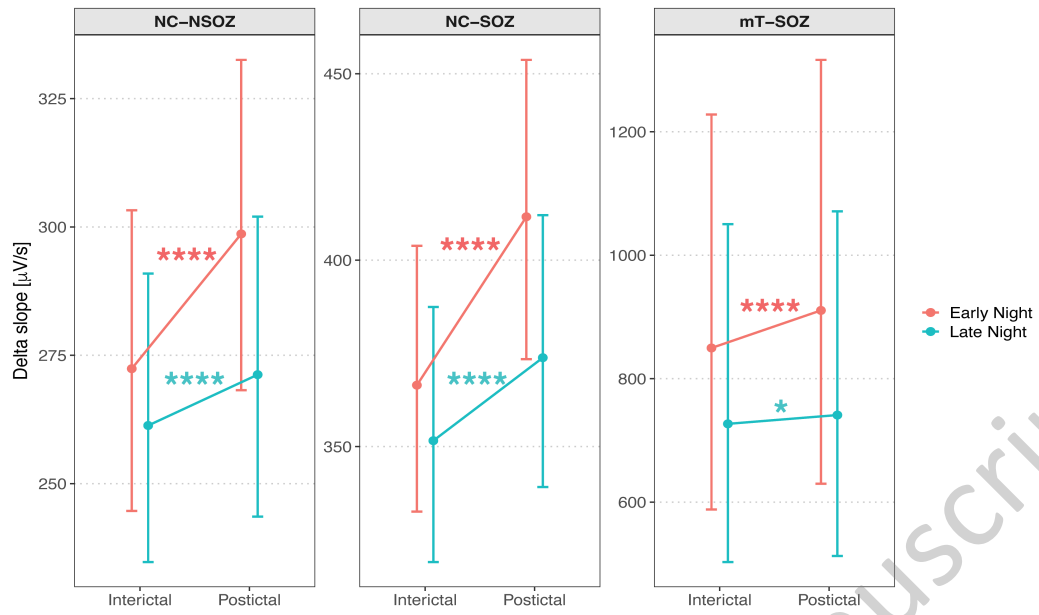


JNeurosci Accepted Manuscript

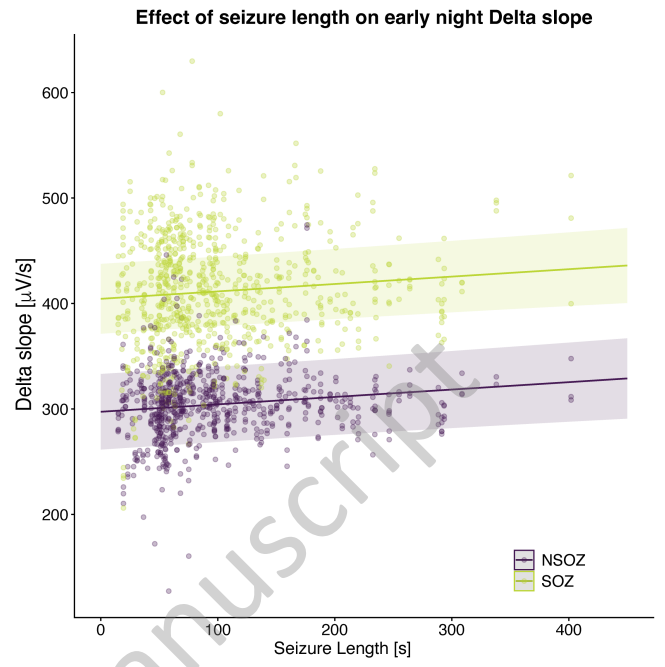
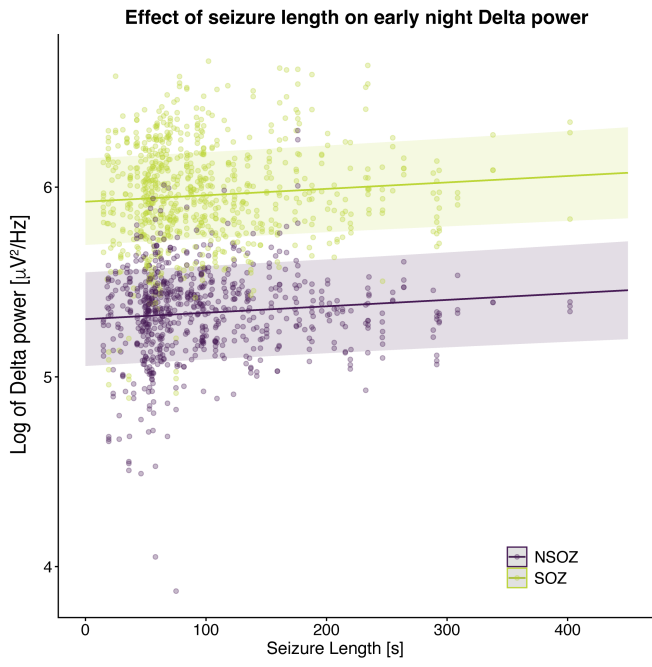




JNeurosci Accepted Manuscript

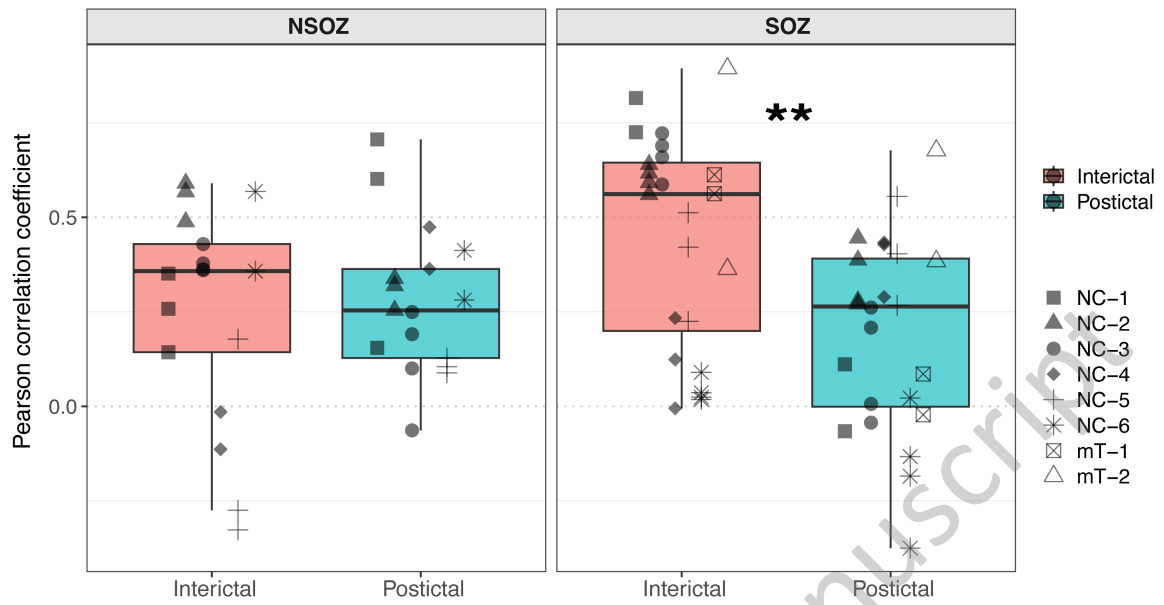


JNeurosci Accepted Manuscript



JNeurosci Accepted Manuscript

### Correlation of postictal delta power with SWA Power



### Correlation of postictal delta power with SWA Slope

